Iso-structural phase transition in $YMnO_3$ nanosized particles

Saurabh Tripathi[a] and Valeri Petkov
Department of Physics, Central Michigan University, Mount Pleasant, Michigan 48859, USA

(Received 17 November 2012; accepted 28 January 2013; published online 13 February 2013)

Structure studies on multiferroic $YMnO_3$ particles with size varying between 467 ± 42 nm (bulk) and 28 ± 3 nm was carried out using high-energy synchrotron x-ray diffraction. Analysis of the diffraction data reveals that when the particles size decreases to about 121 nm an iso-structural phase transition takes place. The transition is accompanied by a substantial change in the unit cell volume and the ratio (c/a) of the parameters of the hexagonal lattice of $YMnO_3$. The phase transition is similar to the one reported in bulk $YMnO_3$ heated to temperatures of about 920 K. In this letter, we argue that the phase transition in nanosized $YMnO_3$ is of an order-disorder type. © *2013 American Institute of Physics*. [http://dx.doi.org/10.1063/1.4791596]

Multiferroics have received enormous attention due to the coexistence of magnetically and ferroelectrically ordered states and the magnetoelectric phenomena arising from the coupling between these two. The coupling allows controlling of the magnetic properties by an application of an electric field and vice versa.[1–4] As a result, it provides an additional degree of freedom in designing actuators, sensors, and data storage devices. Understanding the atomic-scale structure of multiferroics when reduced to nanosized dimensions has become increasingly important with the current advancement of nanotechnology. It is also intriguing from fundamental point of view. An archetypal example of a multiferroic material is $BiFeO_3$. This material shows a strain induced structural transformation where the crystal retains its monoclinic symmetry (Cc) but the ratio (c/a) of the lattice parameters changes abruptly.[5] Recently, an electric-field induced phase transition (Cc-Cc) has been observed in $BiFeO_3$.[6] Such phase transitions are known as iso-structural since the underlying crystal structure symmetry of the material does not change. In general, iso-structural phase transitions are accompanied by anomalous changes in various physical properties such as specific heat, dielectric constant, *etc.*[7–9] Pressure induced iso-structural phase transitions have also been observed.[10] It is not obvious though how to select the order parameter of iso-structural phase transitions. Different order parameters such as defect concentration, atomic positions, compressibility, bond angles, cell volume, and lattice parameters have been suggested.[5,11] The choice of the latter two has been prompted by the observation of an anomalous change of the unit cell volume and the ratio of the lattice constants (c/a) occurring while the underlying space group symmetry remains intact.[12] Recently, a temperature induced iso-structural phase transition was observed with another potentially important Pb and Bi free multiferroic material—$YMnO_3$. It has potential applications in electronic devices such a sensors and non-volatile random access memories[2,3,13,14] Bulk $YMnO_3$ exhibits spontaneous ferroelectric polarization below $Tc_{FE} \approx 930$ K.[15] Additionally, it shows an antiferromagnetic ordering below the Néel temperature T_N of 70 K.[16] At room temperature, bulk $YMnO_3$ is hexagonal and may be well viewed as a stack of disconnected layers of MnO_5 polyhedra with Y atoms positioned between those layers[17,18] (S.G. $P6_3cm$: a_{FE}, c_{FE}) (see Figure 1). The volume of the unit cell is three times that of the high temperature centrosymmetric phase (S.G. $P6_3/mmc$: a_{PE}, c_{PE}) that exhibits paraelectric properties. The lattice parameters of these two phases relate to each other as follows: $a_{FE} = \sqrt{3}\, a_{PE}$ and $c_{FE} = c_{PE}$.[18] The ferroelectric phase is related to the high temperature paraelectric phase by an antiferrodistortive transition taking place at $Tc_{AFD} \sim 1270$ K.[15] The paraelectric to ferroelectric transition temperature Tc_{FE} is somewhat lower than Tc_{AFD}.[1] The onset of the ferroelectric order in $YMnO_3$ is accompanied by buckling of the layers of MnO_5 polyhedra

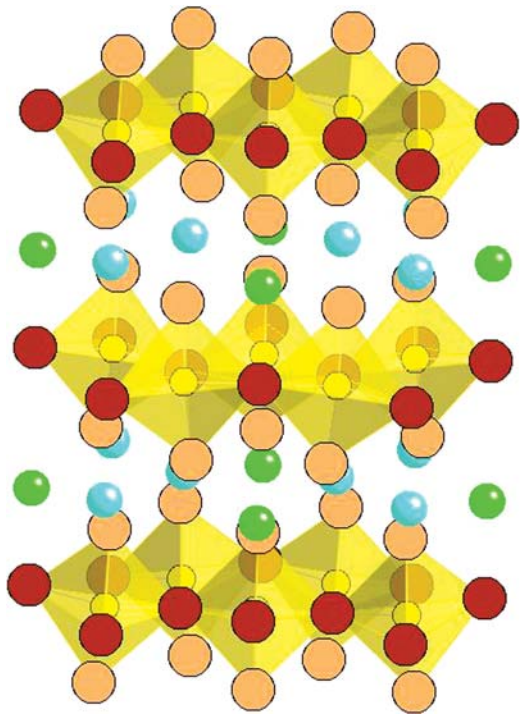

FIG. 1. Room temperature structure of $YMnO_3$ featuring layers of MnO_5 polyhedra (yellow) and two types of Y atoms (blue and green) in between the layers. Apical and basal oxygen atoms are in orange and brown, respectively.

[a]Author to whom correspondence should be addressed. Electronic mail: tripa1s@cmich.edu.

and displacement of the Y ions leading to a net electric polarization.[1] This transition does not involve a change in the crystal symmetry and so can be characterized as an iso-structural phase transition that is of an order-disorder type.[18] In the present work, we study the atomic-scale structure of $YMnO_3$ as a function of particles size using synchrotron X-ray diffraction (SXRD) data. We found that nanosized $YMnO_3$ exhibits an iso-structural phase transition due to the appearance of structural disorder induced by finite size confinement effects. According to the uncertainty principle such a confinement of particles to nanosized dimensions would lead to a gradual increase of the root mean square (rms) fluctuation of atoms about their average positions in the crystalline lattice.[19]

The samples we investigated were prepared by an aqueous chemical synthesis route described elsewhere.[20,21] The cation stoichiometry was controlled through thermogravimetric determination of the cation concentrations of the Y and Mn precursor solutions used in the synthesis to ensure a 1:1 ratio of Y and Mn. The oxygen stoichiometry of $YMnO_3$ is determined by the thermal history, the temperature, and partial pressure of oxygen at the synthesis conditions. Thermogravimetric measurements showed that $YMnO_3$ is oxygen stoichiometric under the synthesis conditions used to prepare the materials investigated in the present work.[21,22]

Synchrotron x-ray diffraction (XRD) experiments were carried out at the 11-ID-C beamline at the Advanced Photon Source using x-rays with energy of 115.232 keV ($\lambda = 0.1076$ Å) and a large-area (mar345) detector.

Rietveld analysis of the synchrotron powder diffraction data was carried out using the program Fullprof.[22] Pseudo-Voigt function was used to define the SXRD peak profiles in the refinements. The SXRD peak profile parameters, the lattice constants, atomic coordinates, and thermal parameters were refined.

Fig. 2 shows the evolution of the SXRD patterns for $YMnO_3$ with decreasing particle size (x), where $x = 470$, 171, 121, 49, 38, and 28 nm. The SXRD patterns show two types of Bragg peaks: peaks due to the underlying hexagonal ($P6_3/mmc$) symmetry of $YMnO_3$ and super-lattice peaks. The latter arise from the tilting of the MnO_5 polyhedra and the antiparallel displacement of Y atoms. The supercell (antiferrodistortive phase) of $YMnO_3$ results from a hardening of a soft zone boundary (K_3: $q = 0\ 0\ 1/3$) mode which causes a tripling of the cell but does not lead to an overall polarization.[1] The ferroelectricity in the cell arises due to a hardening of soft zone center (Γ_1: $q = 0\ 0\ 0$) phonon modes leading to identical displacements of Y atoms in each unit cell and overall polarization.[1] The (102) super-lattice SXRD peak is marked with a dashed line in Fig. 2. The intensity of this peak diminishes as the size of $YMnO_3$ particles decreases. A similar effect has been observed for bulk $YMnO_3$ with increasing temperature.[18] In the latter case, the intensity decrease is due to the increasing thermal disorder in the material.[18] In order to have a clear understanding of the evolution of the super-lattice peak, we have shown it on an enlarged 2θ scale in the inset of Fig. 2. The peak is seen to survive down to particle sizes of 28 nm. Evidently, the crystal structure of nanophase $YMnO_3$ retains the $P6_3mc$ symmetry down to $x = 28$ nm, where the crystallinity gradually

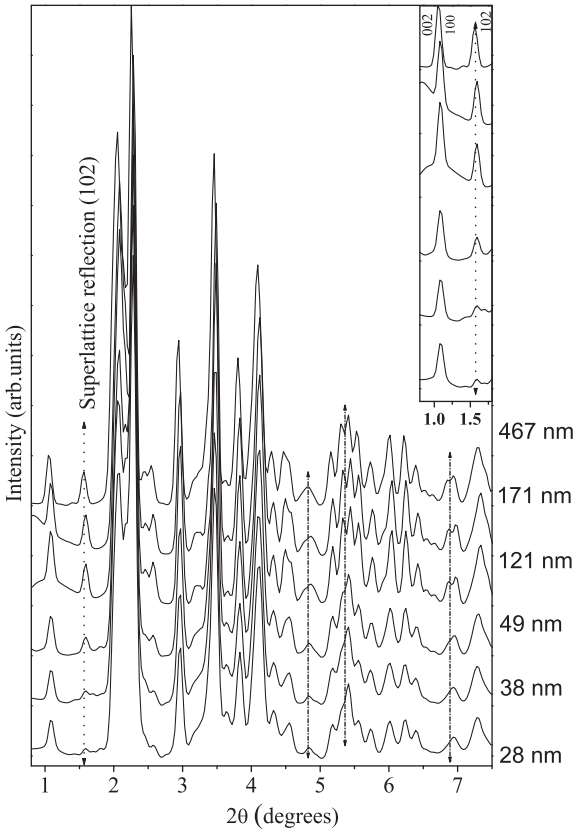

FIG. 2. Synchrotron x-ray diffraction patterns of $YMnO_3$ for various particle size ranging from 470 ± 40 nm to 28 ± 3 nm in size. For clarity, only the low-angle portion of the SXRD patterns is shown (see Ref. 21). The inset shows the evolution of superlattice (102) Bragg reflection.

decays with deceasing particles size so the sample below 28 nm are nanocrystalline in nature. The parameters of the hexagonal lattice and the volume of the hexagonal unit cell, however, evolve not quite in line with diminishing particles size. The evolution of the lattice parameters (a_{FE}, c_{FE}) and their ratio (c_{FE}/a_{FE}) with particles size is shown in Fig. 3. As can be seen in the figure (a_{FE}, c_{FE}) and c_{FE}/a_{FE} show an anomaly around $x = 121$ nm. The c_{FE}/a_{FE} increases when x decreases from 470 to 121 nm and then abruptly decreases with further decreasing x, indicating an iso-structural phase transition. The signature of variation of the lattice constants and their ratio is marked with a dashed-dotted line in Fig. 3. Though this phase transition is of a different origin, it is similar to the temperature driven iso-structural phase transition in bulk $YMnO_3$ observed by Gibbs *et al.*[18] Gibbs *et al.* have shown evidence that the iso-structural phase transition in bulk $YMnO_3$ at high temperatures is due to thermal disorder.[18] Anomalies in the displacements of oxygen atoms, Y-O bond length, and the amplitude of various distortive phonon modes confirm the transition in bulk $YMnO_3$.[18] The ferroelectric polarization calculated from a simple ionic model also reveals an anomaly at approximately 920 K.[18]

The variation of the unit cell volume $V_H = a_H{}^2 c_H(\sqrt{3}/2)$ as obtained from the Rietveld refinements is shown in Fig. 4. The anomalous behavior of the cell volume at particle size of approximately 121 nm also suggests the presence of an iso-structural phase transition. Signatures of an iso-structural phase transition are also seen in the evolution of position of Y atoms with particles size. As shown in Fig. 5, the relative

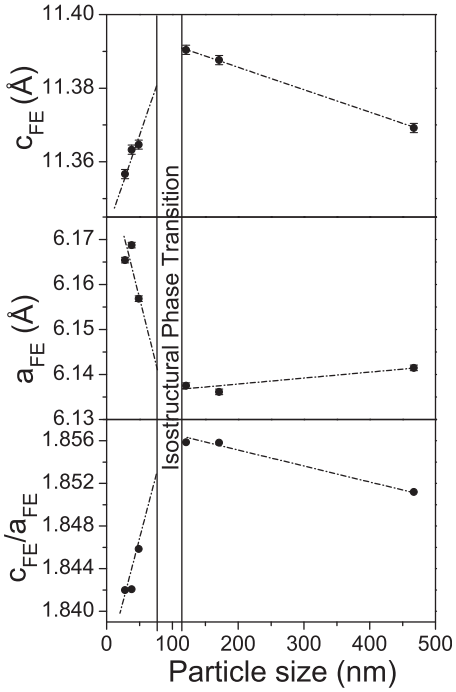

FIG. 3. Evolution of the hexagonal cell parameters (a_{FE}, c_{FE}) of $YMnO_3$ and their ratio with particles size as obtained from Rietveld fits to the synchrotron x-ray diffraction data. Error bars are within the size of symbols.

displacements of Y atoms, $2*dY_1 + 4*dY_2$, from their average positions in the hexagonal lattice[21] shows an anomaly at a particles size of 121 nm. Here dY_1 and dY_2 are the z displacements of the two unequivalent Y atoms in $YMnO_3$. The quantity $2*dY_1 + 4*dY_2$ can be defined as an order parameter of the iso-structural phase transition. Also, it is a measure of the ferroelectricity[21] as the Y atoms displacements play a major role in determining the ferroelectric polarization. The abrupt change of $2*dY_1 + 4*dY_2$ at 121 nm indicates an abrupt change in the ferroelectricity. Thus similarly to the temperature driven iso-structural phase transition in bulk $YMnO_3$ observed by Gibbs *et al.*,[18] a phase transition is observed with nanosized $YMnO_3$ when the particles size is reduced to about 121 nm. Recent studies have also shown a change in the antiferromagnetic transition temperature with decreasing particles size of $YMnO_3$.[23] Thus, we find a change in the physical properties associated with the iso-structural phase transition induced by quantum confinement effects.

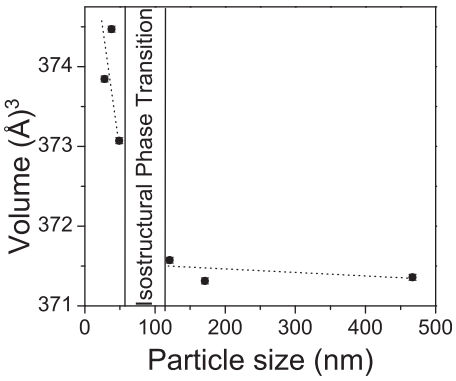

FIG. 4. Evolution of the volume of the hexagonal cell of $YMnO_3$ with particle size as obtained from Rietveld fits to the synchrotron x ray diffraction patterns (see Ref. 21). Error bars are within the size of symbols.

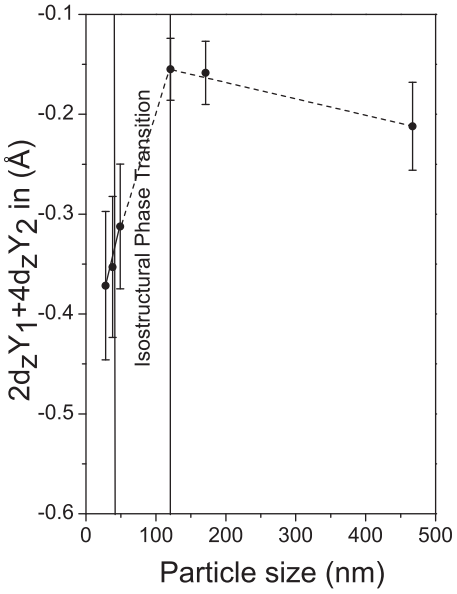

FIG. 5. Evolution of Y atoms displacements as order parameter OP = 2*d_z(Y1) + 4*d_z(Y2) with particle size (see Ref. 21).

In summary, high-energy SXRD studies reveal an iso-structural phase transition with the reduction of particle size in $YMnO_3$. The phase transition has striking similarities with the high temperature phase transition of bulk $YMnO_3$ at ~920 K.

However, in nanosized $YMnO_3$ it is driven not by thermal but by structural disorder due to the confinement of $YMnO_3$ particles to very small dimensions.

We thank S. M. Selbach, K. Bergum, M.-A. Einarsrud, and T. Grande for providing us with high quality samples. Use of the Advanced Photon Source is supported by the Office of Basic Energy Sciences of the U.S. Department of Energy under Contract No. W-31-109-Eng-38.

[1]B. B. Van Aken, T. T. M. Palastra, A. Filippetti, and N A. Spaldin, Nat. Mater. **3**, 164 (2004).
[2]R. Ramesh and N. A. Spaldin, Nature Mater. **6**, 21(2007).
[3]S. W. Cheong and M. Mostovoy, Nature Mater. **6**, 13 (2007).
[4]W. Eerenstein, N. D. Mathur, and J. F. Scott, Nature(London) **442**, 759 (2006).
[5]R. J. Zeches, M. D. Rossell, J. X. Zhang, A. J. Hatt, Q. He, C.-H. Yang, A. Kumar, C. H. Wang, A. Melville, C. Adamo, G. Sheng, Y.-H. Chu, J. F. Ihlefeld, R. Erni, C. Ederer, V. Gopalam, L. Q. Chen, D. G. Scholm, N. A. Spaldin, L. W. Martin, and R. Ramesh, Science **326**, 977 (2009).
[6]S. Lisenkov, D. Rahmedov, and L. Bellaiche, Phys. Rev. Lett. **103**, 047204 (2009).
[7]K. Gesi, J. Phys. Soc. Jpn. **43**, 1941, (1977).
[8]E. R. Magnaschi, A. Rigamonti, and L. Menafra, Phys. Rev. B **14**, 2005 (1976).
[9]V. E. Schneider and E. E. Tornau, Phys. Status Solidi (b) **111**, 565 (1982).
[10]A. Alavi, A. Y. Lozovoi, and M. W. Finnis, Phys. Rev. Lett. **83**, 979 (1999).
[11]V. Ranjan, S. Bin-Omran, L. Bellaiche, and A. Alsaad, Phys. Rev. B **71**, 195302 (2005); S. Tripathi, Ph. D. Thesis, "Phase Transition Studies on the Mixed (1−x)$NaNbO_3$−x$CaTiO_3$ System," Banaras Hindu University (2012); S. Bhattacharjee, K. Taji, C. Moriyoshi, Y. Kuroiwa, and D. Pandey, Phys. Rev. B. **84**, 104116 (2011); A. Singh, V. Pandey, R. K. Kotnala, and D. Pandey, Phys. Rev. Lett. **101**, 247602 (2008).
[12]J. F. Scott, Adv Mater. **22**, 2106 (2010).
[13]N. Fujimura, T. Ishida, T. Yoshimura, and T. Ito, Appl. Phys. Lett. **69**, 1011 (1996).
[14]N. Fujimura, S.-I. Azuma, N. Aoki, T. Yoshimura, and T. Ito, J. Appl. Phys. **80**, 7084 (1996).

[15]I. G. Ismailzade and S. A. Kizhaev, Sov. Phys. Solid State **7**, 236 (1965).
[16]D. G. Tomuta, S. Ramakrishnan, G. J. Nieuwenhuys, and J. A. Mydosh, J. Phys.: Condensed Matter **13**, 4543 (2001).
[17]H. L. Yakel, W. C. Koehler, E. F. Bertaut, and E. F. Forrat, Acta Crytallogr. **16**, 957 (1963).
[18]A. S. Gibbs, K. S. Knight, and P. Lightfoot, Phys. Rev. B **83**, 094111 (2011).
[19]V. Petkov, V. Buscaglia, M. T. Buscaglia, Z. Zhao, and Y. Ren, Phys. Rev. B **78**, 054107 (2008).
[20]K. Bergum, H. Okamoto, H. Fjelvag, T. Grande, and M.-A. Einarsrud, and S. M. Selbach, Dalton Trans. **40**, 7583(2011).
[21]S. Tripathi, V. Petkov, S. M. Selbach, K. Bergum, M.-A. Einarsrud, T. Grande, and Y. Ren, Phys. Rev. B **86**, 094101 (2012).
[22]J. Rodríguez-Carvajal, Physica B **192**, 55 (1993).
[23]T.-C. Han, W.-L. Hsu, and W.-D. Lee, Nanoscale Res. Lett. **6**, 201 (2011).